N90-12795

Frame Synchronization Methods Based on Channel Symbol Measurements

S. Dolinar and K.-M. Cheung

Communications Systems Research Section

The current DSN frame synchronization procedure is based on monitoring the decoded bit stream for the appearance of a sync marker sequence that is transmitted once every data frame. This article explores the possibility of obtaining frame synchronization by processing the raw received channel symbols rather than the decoded bits. Performance results are derived for three channel symbol sync methods, and these are compared with results for decoded bit sync methods reported elsewhere. It is shown that each class of methods has advantages or disadvantages under different assumptions on the frame length, the global acquisition strategy, and the desired measure of acquisition timeliness.

It is shown that the sync statistics based on decoded bits are superior to the statistics based on channel symbols, if the desired operating region utilizes a probability of miss many orders of magnitude higher than the probability of false alarm. This operating point is applicable for very large frame lengths and minimal frame-to-frame verification strategy. On the other hand, the statistics based on channel symbols are superior if the desired operating point has a miss probability only a few orders of magnitude greater than the false alarm probability. This happens for small frames or when frame-to-frame verifications are required. Among the three channel symbol methods examined, the squared-distance statistic offers the best performance in the range of normal signal-to-noise ratios, but it degrades more rapidly than the correlation statistic or the hard-limited symbol discrepancy count statistic when the signal-to-noise ratio is extremely low.

I. Introduction

The current DSN frame synchronization procedure is based on transmitting from the spacecraft a convolutionally encoded 32-bit sync marker sequence at the beginning of every data frame consisting of around 10^4 bits. On the ground, the decoded bit stream is monitored for a 32-bit window of agreements with the marker, and a likely sync location is identified by comparing the number of disagreements with a preselected threshold. In addition, a frame-to-frame verification strategy is employed to definitively declare sync acquisition or sync loss.

This article explores the possibility of obtaining frame synchronization by processing the raw received channel symbols rather than the decoded bits. Performance results are derived for three channel symbol sync methods, and these are compared with results for decoded bit sync methods reported elsewhere [1, 2]. It is shown that each class of methods has advantages or disadvantages under different assumption on the frame length, the global acquisition strategy, and the desired measure of acquisition timeliness.

II. Various Possible Synchronization Methods

A. General Framework for a Wide Class of Synchronization Methods

The DSN's current method of frame synchronization can be viewed as a prototype of a fairly general type of synchronization scheme. There are three basic levels to this scheme. First, a statistic x is measured at all possible locations of the frame marker, and the observed values of x are used to identify likely locations of the marker. Second, values of x obtained at all possible locations within a frame and for different frames are correlated for one or more frames to verify and select the most likely marker location. Third, the statistic x is monitored from frame to frame at the selected marker location to verify continued sync.

This three-level synchronization model can be completely general if the decisions at all three levels can depend in an arbitrary way on all the observed data. In practice, it is usually assumed for ease of implementation that the three levels of decisions are mostly decoupled. This article considers only the first two levels, with primary emphasis on the first level.

Ideally, the statistic x should be a sufficient statistic summarizing all the relevant information in the data. In practice, x is constrained to be a meaningful, but easy to compute, measure of the data. There are many possible choices for the statistic x. This statistic may be based directly on observation of the received channel symbols, or it may be calculated from the decoded output of the Viterbi decoder. This article analyzes several different statistics based on channel symbol measurements, and briefly discusses some other statistics based on decoded bits; these statistics are reported elsewhere [1, 2].

Figure 1 is a general system diagram introducing notation for describing the two types of synchronization statistics. The stream of incoming "data" bits $\{b_i\}$ includes both true data bits and sync marker bits $\{\lambda_i\}$. The "data" bit stream is packaged into data frames $\{b_i, i = 1, \ldots, B\}$ of B bits each, and L sync marker bits $\{\lambda_i, i = 1, \ldots, L\}$ are included in every data frame. The "data" bit stream is convolutionally encoded by a rate $1/N$, constraint length K convolutional encoder. The encoded channel symbol stream $\{s_i, i = 1, \ldots, S\}$ is likewise partitioned into frames of $S = NB$ symbols each, and each frame includes a set of $M = N(L - K + 1)$ sync marker symbols $\{m_i, i = 1, \ldots, M\}$ that are totally determined by the sync marker bits $\{\lambda_i, i = 1, \ldots, L\}$. The remaining $N(B - L + K - 1)$ symbols in each frame are dependent solely on the true data bits or else on a combination of true data bits and sync marker bits.

The channel symbols are assumed to have constant magnitude s (i.e., $s_i = \pm s$), and they are received in additive white Gaussian noise $\{n_i, i = 1, \ldots, S\}$ with zero mean and variance σ^2. The ratio $\rho = s^2/\sigma^2$ is a signal-to-noise parameter. In terms of ρ, the channel symbol signal-to-noise ratio is $E_s/N_0 = \rho/2$, and the bit-energy-to-noise ratio is $E_b/N_0 = N\rho/2$. The received symbols $\{r_i, i = 1, \ldots, S\}$ are passed through a maximum likelihood convolutional decoder (Viterbi decoder) to obtain the decoded bits $\{d_i, i = 1, \ldots, B\}$.

The general performance expressions in this article are derived for arbitrary combinations of the parameters K, N, L, M, B, and S. However, all explicit performance curves assume a 32-bit marker sequence and the NASA-standard constraint length 7, rate 1/2 code (i.e., $L = 32$,

$M = 52$, $K = 7$, and $N = 2$). The curves in Section III are applicable to any frame length, while the curves in Section IV assume a frame length of 10000 bits or 20000 symbols (i.e., $B = 10000$, $S = 20000$).

B. Sync Methods Based on Decoded Bits

Frame sync observables based on decoded bits are a function of the L-vector of discrepancies $\{\lambda_i \oplus d_i, \ i = 1,\dots,L\}$ between the sync marker bits $\{\lambda_i, \ i = 1,\dots,L\}$ and a sliding L-bit window of actual decoded bits $\{d_i, i = 1,\dots,L\}$. Several reasonable statistics are described in this section. Further analysis of observables based on decoded bits is not carried out in this article, but performance curves are cited from [1, 2] for comparison with channel symbol methods.

1. Decoded Bit Discrepancy Count Statistic. In this case, the statistic x simply counts the number of discrepancies between the sync marker bits and the current L-bit window:

$$x = \sum_{i=1}^{L} [\lambda_i \oplus d_i]$$

This is the statistic used in the current DSN frame sync algorithm.

2. Decoded Bit Discrepancy Span Statistic. Viterbi decoders tend to make bursts of errors and the decoded bits are essentially random inside an error burst [3]. Thus, any agreements with the sync marker that occur inside a decoder error burst are completely accidental and should not be counted as true agreements. This observation leads to the definition of the discrepancy span statistic. The discrepancy span measures the distance in bits between the first and last disagreements with the sync marker. The statistic x is defined simply by

$$x = i_2 - i_1 + 1$$

where

$$i_1 = \min_{1 \le i \le M} \{i : (\lambda_i \oplus d_i) = 1\}$$

$$i_2 = \max_{1 \le i \le M} \{i : (\lambda_i \oplus d_i) = 1\}$$

This statistic was first suggested and analyzed in [2].

C. Sync Methods Based on Channel Symbols

Frame sync observables based on channel symbols are obtained by comparing a sliding M-symbol window of received symbols $\{r_i, i = 1,\dots,M\}$ with the sync marker symbols $\{m_i, i = 1,\dots M\}$. Several reasonable channel symbol statistics are described in this section.

1. Hard-Limited Channel Symbol Discrepancy Count. The channel symbol statistic most similar to the decoded bit statistics is obtained by hard limiting each received symbol r_i to the nearest transmitted symbol value $\pm s$ and counting disagreements with the sync marker sequence. A statistic x that simply counts the number of discrepant symbols is defined by

$$x = \frac{1}{2} \sum_{i=1}^{M} [1 - \text{sgn}\,(m_i)\,\text{sgn}\,(r_i)]$$

This statistic x counts one discrepancy for every disagreement in sign between a received symbol r_i and the corresponding sync marker symbol m_i.

Because the received symbols $\{r_i\}$ contain white Gaussian noise and are not prone to error bursts, burst-inspired statistics such as the discrepancy span statistic are not useful in the channel symbol domain. However, statistics that make use of the soft-quantized information in the channel symbols can offer improvement.

2. Weighted Symbol Discrepancies. An interesting statistic using soft-quantized information is derived as a weighted sum of symbol discrepancies. The statistic x is defined by

$$x = \sum_{i=1}^{M} \max\,[0, -r_i\,\text{sgn}\,(m_i)]$$

Just like the hard-limited symbol discrepancy count statistic, this statistic x counts 0 every time the received symbol r_i and the corresponding sync marker symbol m_i agree in sign, no matter how inexact the agreement might be. However, this statistic does not count all sign discrepancies equally, but instead weights them by the magnitude of the corresponding received symbols.

The weighted symbol discrepancy statistic was first proposed by Massey [4] as a good approximation to the maximum likelihood detection statistic in the region of high signal-to-noise ratio. This statistic is not further analyzed in this article, but will be examined in the future by simulation or central limit theorem approximation.

3. Channel Symbol Correlation Statistic.

One natural soft-quantized statistic measures the correlation between the received symbols and the sync marker symbols. The statistic x is defined by

$$x = \sum_{i=1}^{M} m_i(m_i - r_i)$$

The observed value of this statistic should be near 0 if $\{r_i, \; i = 1, \ldots, M\}$ contains the marker, and otherwise should be a large positive number around Ms^2. With this definition, the correlation statistic exhibits the same qualitative behavior as the discrepancy-based statistics.

4. Channel Symbol Squared Distance Statistic.

Another natural symbol-based statistic measures the squared distance between the received symbols and the sync marker symbols. The statistic x is defined by

$$x = \sum_{i=1}^{M} (m_i - r_i)^2$$

Again, a small value of x indicates agreement with the marker, while a large value indicates disagreement.

III. Probability of Miss and Probability of False Alarm

A. Basic Definitions

All of the statistics x defined in the previous section are scalar; a value of x near 0 indicates a match with the sync marker, while a large positive value indicates disagreement. Thus, it is natural to use the observed values of x to make tentative yes–no decisions about the location of the marker, according to whether x falls below or exceeds

a threshold θ. The tentative decision rule for all statistics defined above is of the general form

$$x \underset{\substack{> \\ \text{no sync}}}{\overset{\substack{\text{sync} \\ \leq}}{}} \theta$$

If x exceeds θ when x is measured at the true position of the marker, the tentative decision rule results in the true marker location being missed in the current frame. Conversely, if x falls below θ when x is not measured at the true marker position, then the decision rule causes a false detection of sync or false alarm.

The intrinsic goodness of various statistics x can be evaluated by comparing the tradeoff between probability of miss (P_M) and probability of false alarm (P_F), which results as the threshold θ is varied for a given statistic x. The miss probability and false alarm probability are defined as

$$P_M = \text{Prob } [x > \theta| \text{ sync marker located at}$$
$$\text{current } L\text{-bit or } M\text{-symbol window}]$$

$$P_F = \text{Prob } [x \leq \theta| \text{ sync marker not located at}$$
$$\text{current } L\text{-bit or } M\text{-symbol window}]$$

The miss probability P_M is the probability that the true marker will fail to pass the threshold test at the true location of the marker. Within any one data frame, there is only one opportunity for a miss to occur. The false alarm probability P_F is the probability that the threshold test will be passed at some particular location that contains only true data bits and symbols or possibly a combination of true data bits and symbols and marker bits and symbols. In each frame there are $B-1$ opportunities for false alarm for algorithms based on decoded bits, or $S-1$ opportunities for algorithms based on channel symbols.

B. Computation of P_M versus P_F for Various Observables

1. Decoded Bit Discrepancy Count Statistic.

The tradeoff between miss probability and false alarm probability for the decoded bit discrepancy count statis-

tic has been reported in [1, 2]. A graph showing some of the results of [2] is presented in Fig. 2.

It must be noted that the miss probability and false alarm probability defined in [2] are not equal to those used in this article. In [2], the threshold test had to be passed at the same location in two consecutive frames for either a false alarm or detection of true sync to occur. The false alarm probability $(O|M')$ and miss probability $1 - P(O|M)$ defined in [2] are related to the corresponding probabilities P_F and P_M used in this article as $P(O|M') = P_F^2$, $1 - P(O|M) = 1 - (1 - P_M)^2$.

2. Decoded Bit Discrepancy Span Statistic.

The miss probability versus false alarm probability curves for the decoded bit discrepancy span statistic are shown in Fig. 3. These curves are taken from [2], after adjusting for the different definitions of miss probability and false alarm probability described above.

3. Hard-Limited Channel Symbol Discrepancy Count Statistic.

Measured at the marker, the hard-limited symbol discrepancy count statistic x is a binomial random variable,

$$x = \sum_{i=1}^{M} \frac{1}{2} \left[1 - \text{sgn}\,(m_i)\, \text{sgn}\,(m_i + n_i) \right] = \sum_{i=1}^{M} x_i$$

where $\{x_i, i = 1, \ldots, M\}$ are independent binary random variables,

$$\text{Prob}\,[x_i = 1] = q = 1 - \text{Prob}\,[x_i = 0]$$

with

$$q = \text{Prob}\,[n_i > m] = Q\left(\frac{m}{\sigma}\right) = Q(\sqrt{\rho})$$

and

$$Q(u) = \frac{1}{\sqrt{2\pi}} \int_u^{\infty} e^{-t^2/2} dt$$

The probability distribution for the statistic x is given by

$$\text{Prob}\,[x = j] = \binom{M}{j} q^j (1 - q)^{M-j}, \quad j = 0, \ldots, M$$

The miss probability is easily evaluated as

$$P_M = \sum_{j=\theta+1}^{M} \binom{M}{j} q^j (1 - q)^{M-j}$$

At any given location not overlapping the marker, the statistic x is conditionally a sum of two binomial random variables whose statistics depend on the discrepancies $\{\delta_i, i = 1, \ldots, M\}$ between the marker symbols $\{m_i, i = 1, \ldots, M\}$ and the sliding window of M symbols $\{s_i, i = 1, \ldots, M\}$ at the current location

$$\delta_i = \frac{1}{2} \left[1 - \text{sgn}\,(m_i)\, \text{sgn}\,(s_i) \right], \quad i = 1, \ldots, M$$

Then, if w is the Hamming weight of the discrepancy sequence $\{\delta_i, i = 1, \ldots, M\}$,

$$w = \sum_{i=1}^{M} \delta_i$$

the statistic x can be written as

$$x = \sum_{i=1}^{M-w} \frac{1}{2} \left[1 - \text{sgn}\,(m_i)\, \text{sgn}\,(m_i + n_i) \right]$$

$$+ \sum_{i=1}^{w} \frac{1}{2} \left[1 - \text{sgn}\,(m_i)\, \text{sgn}\,(-m_i + n_i) \right]$$

$$= \sum_{i=1}^{M-w} x_i + \sum_{i=1}^{w} y_i$$

where $\{x_i, i = 1, \ldots, M - w\}$ are independent binary random variables as defined above and $\{y_i, i = 1, \ldots, w\}$ are

also independent binary random variables with a different probability,

$$\text{Prob}\,[y_i = 1] = p = 1 - \text{Prob}\,[y_i = 0]$$

$$p = 1 - Q\left(\frac{m}{\sigma}\right) = 1 - q$$

The probability of false alarm is obtained by averaging the conditional probability that x will fall below threshold over the possible discrepancy weights w,

$$P_F = \sum_{w=0}^{M} \text{Prob}[w]$$

$$\times \sum_{\substack{j=0 \\ j+k \le \theta}}^{M-w} \sum_{k=0}^{w} \binom{M-w}{j} q^j \,(1-q)^{M-w-j}$$

$$\times \binom{w}{k} p^k \,(1-p)^{w-k}$$

The discrepancy weight probability distribution $\text{Prob}[w]$ was obtained by exhaustive enumeration for a 32-bit sync marker sequence and the NASA-standard constraint length 7, rate 1/2 convolutional code. This distribution is approximately binomial except at the tails (w near 0 or M). The exact distribution for the NASA-standard code is reported in Appendix A.

The tradeoff between miss probability and false alarm probability for the hard-limited channel symbol discrepancy count statistic is plotted in Fig. 4 for signal-to-noise ratios E_b/N_0 ranging from -1.5 dB to $+3.0$ dB.

4. Channel Symbol Correlation Statistic. Measured at the marker, the channel symbol correlation statistic x is a sum of independent Gaussian random variables,

$$x = \sum_{i=1}^{M} (-m_i n_i) = \sum_{i=1}^{M} u_i$$

where u_i is $N(0, s^2\sigma^2)$, x/σ^2 is $N(0, Ms^2/\sigma^2) = N(0, M\rho)$. Thus, the miss probability is calculated simply as

$$P_M = Q\left(\frac{\theta}{\sqrt{M}s\sigma}\right) = Q\left(\frac{\theta/\sigma^2}{\sqrt{M}\rho}\right)$$

Away from the marker, the correlation statistic x is a sum of conditionally Gaussian random variables, some with zero mean and some with nonzero mean:

$$x = \sum_{i=1}^{M-w} (-m_i n_i) + \sum_{i=1}^{w} (2m_i^2 - m_i n_i)$$

$$= \sum_{i=1}^{M-w} u_i + \sum_{i=1}^{w} v_i$$

where v_i is $N(2s^2, s^2\sigma^2)$, x/σ^2 is $N(2ws^2/\sigma^2, Ms^2/\sigma^2) = N(2w\rho, M\rho)$.

The false alarm probability is obtained by averaging the conditional Gaussian probability distribution for x over the discrepancy weight distribution $\text{Prob}[w]$,

$$P_F = \sum_{w=0}^{M} \text{Prob}[w] \, Q\left(\frac{2w\rho - \theta/\sigma^2}{\sqrt{M}\rho}\right)$$

Figure 5 shows P_M versus P_F for the channel symbol correlation statistic.

5. Channel Symbol Squared Distance Statistic. At the marker, the squared distance statistic x is a sum of squares of M zero-mean Gaussian random variables, i.e., x is a chi-squared random variable with M degrees of freedom:

$$x = \sum_{i=1}^{M} n_i^2$$

where n_i is $N(0, \sigma^2)$, x/σ^2 is $\chi^2(M)$. Away from the marker, the squared-distance statistic is conditionally a noncentral chi-squared random variable,

$$x = \sum_{i=1}^{M-w} n_i^2 + \sum_{i=1}^{w} (2m_i - n_i)^2$$

$$= \sum_{i=1}^{M-w} n_i^2 + \sum_{i=1}^{w} z_i^2$$

where z_i is $N(2m_i, \sigma^2)$, x/σ^2 is noncentral $\chi^2(M, 4w\rho)$. The probability distribution functions for central and non-central chi-squared random variables with an even number of degrees of freedom can be related to the probability distributions for certain Poisson random variables, as shown in Appendix B. Assuming that the number of marker symbols M is even, the miss probability and false alarm probability can thus be expressed as

$$P_M = \text{Prob}\left[\sum_{i=1}^{M} n_i^2 > 0\right]$$

$$= \text{Prob}\left[k_1 \leq \frac{M}{2} - 1\right]$$

$$P_F = \sum_{w=0}^{M} \text{Prob}[w] \ \text{Prob}\left[\sum_{i=1}^{M-w} n_i^2 + \sum_{i=1}^{w} z_i^2 \leq \theta\right]$$

$$= \sum_{w=0}^{M} \text{Prob}[w] \ \text{Prob}\left[k_1 - k_2(w) \geq \frac{M}{2}\right]$$

where k_1 is Poisson $(\theta/2\sigma^2)$, $k_2(w)$ is Poisson $(2w\rho)$, and $k_1, k_2(w)$ are conditionally independent given w. Evaluating the Poisson probabilities gives

$$P_M = \sum_{k_1=0}^{\frac{M}{2}-1} \frac{\left(\frac{\theta}{2\sigma^2}\right)^{k_1}}{k_1!} \exp\left(-\frac{\theta}{2\sigma^2}\right)$$

$$P_F = \sum_{w=0}^{M} \text{Prob}[w] \sum_{k_2=0}^{\infty} \frac{(2w\rho)^{k_2}}{k_2!} \exp(-2w\rho)$$

$$\times \sum_{k_1=k_2+\frac{M}{2}}^{\infty} \frac{\left(\frac{\theta}{2\sigma^2}\right)^{k_1}}{k_1!} \exp\left(-\frac{\theta}{2\sigma^2}\right)$$

The resulting curves of P_M versus P_F are plotted in Fig. 6.

C. Conclusions from the P_M versus P_F Curves

Several important conclusions about the relative performance achievable by the various sync statistics can be drawn by comparing the tradeoff curves in Figs. 2 through 6. A P_M versus P_F curve which is uniformly below and to the left of another indicates superiority in the corresponding sync statistic. For example, Figs. 2 and 3 appear to show that the decoded bit discrepancy span statistic is uniformly superior to the decoded bit discrepancy count statistic, although the advantage disappears at small P_F.

Among the channel symbol methods, the squared distance statistic yields superior performance for large E_b/N_0, while the correlation statistic overtakes it for very poor signal-to-noise ratio ($E_b/N_0 < 0.5$ dB). The performance of the hard-limited symbol discrepancy count statistic resembles the correlation statistic's performance, but is decidedly inferior at very low signal-to-noise ratio ($E_b/N_0 < 0$ dB). The theoretically near-optimum weighted symbol discrepancy statistic may be better than all three, but it was not analyzed here.

Comparing the performances of the decoded bit methods with those of the channel symbol methods is a more complicated issue, because the tradeoff curves are dissimilar in shape. The curves for the decoded bit statistics are much flatter than those for the channel symbol statistics. There is a distinct crossover point between the curve for one of the decoded bit statistics and the corresponding curve for one of the channel symbol statistics. To the left of the crossover point (small P_F), the decoded bit statistic is superior, while the channel symbol statistic performs better on the other side (large P_F). The judgment of which statistic is better depends on the desired operating point on the P_M versus P_F curves. As shown in Section IV, this desired operating point is a function of the frame length, the global acquisition strategy, and the preferred measure of acquisition timeliness.

The flatness of the P_M versus P_F curves for the decoded bit statistics is due to the bursty nature of the Viterbi decoder errors. A marker-length section of decoded bits is likely to be either entirely correct or mostly garbage. Thus, only a small improvement in miss probability can be obtained by increasing the threshold θ above 0, while the

false alarm probability increases substantially. The consequence of the flat P_M versus P_F curves is that the performance of the decoded bit schemes is basically limited by the Viterbi decoder's error probability for decoding a 32-bit symbol. Arbitrarily small false alarm probability (down to a minimum of approximately 2^{-L}, the probability that L data bits will accidentally reproduce the sync marker) can be purchased at little expense in P_M. However, reducing P_F too far has no benefit if the frame length is small. The acquisition failure probability is totally dominated by P_M in this case. Even with a large frame, there are other ways to reduce P_F dramatically, such as by requiring frame-to-frame verification before declaring sync. Such a technique has virtually no benefit if P_F can already be made small without it.

While the decoded bit curves are very flat, the channel symbol curves show a lot of elasticity. Appreciable changes in P_F result in appreciable changes in P_M, and vice-versa. These methods show stronger response to frame-to-frame verification strategies. Of course, the increased elasticity also means that all parameters must be more delicately adjusted for optimum behavior.

IV. Probability of Acquisition of True Sync

A. Assumptions About the Acquisition Strategy

The miss probability versus false alarm probability curves reflect the power of a given statistic x to discriminate in a pairwise manner between the true sync marker location and any one of the possible false locations. To compute the probability that sync will be acquired correctly, it is also necessary to consider the global strategy that combines all of the bit-by-bit or symbol-by-symbol tentative decisions based on x to arrive at a declared sync position.

The global strategy can be divided into two parts. First, how are the outcomes of all the tentative decisions within one frame period combined to select or rank the candidate marker locations based on a single frame of observations? Second, are observations from succeeding frames required to reevaluate the candidates from the first frame before declaring sync, and, if so, how are they applied? These two parts may be called the intraframe strategy and the frame-to-frame strategy, respectively.

In this article, it is assumed that no sync candidates emerge from any frame in which the threshold test is failed at all locations; when this happens, the sync search is restarted from scratch in the next frame. If the threshold test is passed at one or more locations within a frame, it is assumed that the *first* such location tested is the unique sync candidate based on that frame's observations. The current DSN sync algorithm can switch between this scheme and another slightly more accurate one that selects the *most probable* location (i.e., the one that passes the threshold test by the widest margin). The latter intraframe strategy is not considered in this article.

Two different frame-to-frame strategies are considered. The simplest frame-to-frame strategy requires no correlation with succeeding frames. Sync is declared or not declared solely on the basis of the intraframe results in a single frame. A second frame-to-frame strategy is one currently used by the DSN, which requires next-frame verification before declaration of sync. In this strategy, the unique sync candidate (if any) from any single frame is chosen as the sync location if and only if it is *verified once* in the next succeeding frame by repassing the threshold test at the corresponding location within that frame.

Each acquisition strategy and sync statistic must be evaluated relative to an appropriate measure of performance. The appropriate performance measure is not necessarily the same for different strategies. For example, minimum acquisition times under an elaborate frame-to-frame verification strategy are guaranteed to be longer than under a single-frame strategy. In this article, the probability of acquisition of true sync in one frame is used to compare the performance of different basic observables x under the single-frame acquisition strategy. On the other hand, the desired measure of performance for the strategy requiring next-frame verification is the probability of acquisition of true sync within *four* frames or less.

B. Probability of Acquisition of True Sync in One Frame

For true sync to be declared after one frame length of observations, the true sync location must pass the threshold test, and no false sync location may pass the threshold test earlier. The probability that the true sync location passes the threshold test is $1 - P_M$. The probability that any particular false sync location passes the threshold test is P_F. As stated earlier, it is assumed that the same false

alarm probability P_F applies both to data-only locations and to locations partially overlapping the marker.

The probability that at least one false sync will be detected before the true sync location is tested can be upper bounded and approximated by multiplying the false alarm probability P_F by the total number of false sync locations tested prior to the true sync location. This number is a random variable that depends on the exact time the synchronization search was started relative to the true frame boundaries. If the synchronization search is started at a random time, the average number of false sync locations tested before the true sync location is $(B-1)/2$ for algorithms based on decoded bits or $(S-1)/2$ for algorithms based on channel symbols.

In summary, true sync can fail to be acquired in one frame if either the true sync location fails the threshold test, or if a false alarm occurs at any of the false sync locations tested earlier. These two events occur with probabilities P_M and $[(B-1)/2]P_F$ or $[(S-1)/2]P_F$, respectively. Thus, the probability of acquisition of true sync within one frame is approximated for small P_M and P_F by

Prob[acquisition of true sync within one frame]

$$\approx 1 - P_M - \frac{B-1}{2}P_F, \quad \text{for algorithms based}$$

on decoded bits

$$\approx 1 - P_M - \frac{S-1}{2}P_F, \quad \text{for algorithms based}$$

on channel symbols

This probability is plotted in Fig. 7 for the five sync observables considered in Figs. 2 through 6, assuming a frame length of 10000 bits or 20000 symbols and an optimized threshold at each signal-to-noise ratio.

C. Probability of Acquisition of True Sync Within Four Frames, With Required Next-Frame Verification

In this section, it is assumed that the frame-to-frame strategy requires that the threshold test be passed at the same location in two consecutive frames before sync is declared. For true sync to be declared within four frames,

the true sync location must pass the threshold test either in the first and second frames, or in the second and third frames after failing to pass in the first frame, or in the third and fourth frames after failing the test in the second frame. These three events happen with probabilities $(1-P_M)^2$, $P_M(1-P_M)^2$, and $P_M(1-P_M)^2$, respectively, assuming that observations are independent from frame to frame. In addition, it is necessary that no false sync location be detected and verified before true sync can be declared. Any particular false sync location is detected and verified on the second frame, third frame, or fourth frame with probabilities P_F^2, $P_F^2(1-P_F)$, or $P_F^2(1-P_F)$, respectively. The corresponding probabilities that at least one false sync is detected and verified on the second frame, third frame, or fourth frame can be upper bounded and approximated by multiplying the former probabilities by the number of possible false sync locations.

To calculate the probability that a false sync declaration might preempt the possibility of declaring true sync, it is necessary to divide the possible false sync locations into two categories. Some false sync locations are first subjected to the threshold test prior to the true sync location, and some are first tested after the true sync location. The first category of false sync locations can preempt a true declaration of sync if both the false declaration and the true declaration occur in the *same* number of frames, while the second category causes trouble only if false sync is declared in *fewer* frames than true sync. If the frame sync process is started at a random point in the frame, the average number of false sync locations in each category is $(B-1)/2$ or $(S-1)/2$.

The dominant contribution to the probability that a false sync will be declared before true sync comes from the probability that false locations in the first category are detected and verified at the first opportunity, i.e., within two frames. This probability is upper bounded and approximated by $[(B-1)/2]P_F^2$ or $[(S-1)/2]P_F^2$. All other contributions to the probability of preemptive declaration of false sync involve terms of order $P_M P_F^2$ and higher-order terms, and these terms are unimportant if both P_M and P_F are small.

The previous observations can be summarized as follows. True sync can fail to be acquired within four frames if the true sync location is not detected and verified within four frames or if a false sync location is detected and verified earlier. The first event happens with probability $1-(1-P_M)^2(1+2P_M) \approx 3P_M^2$, and the second event

happens with approximate probability $[(B-1)/2]P_F^2$ or $[(S-1)/2]P_F^2$. Thus, the probability of true acquisition within four frames is approximated for small P_M and P_F by

Prob [acquisition of true sync within four frames

with one required verification]

$$\approx 1 - 3P_M^2 - \frac{B-1}{2}P_F^2, \quad \text{for algorithms based}$$

on decoded bits

$$\approx 1 - 3P_M^2 - \frac{S-1}{2}P_F^2, \quad \text{for algorithms based}$$
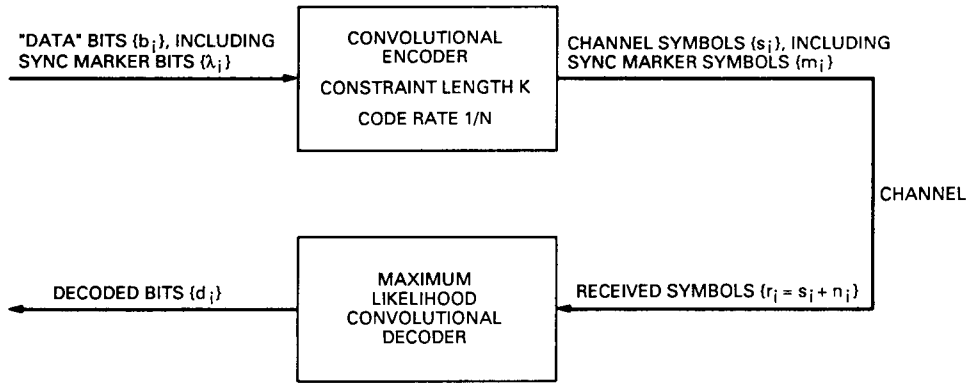
on channel symbols

This probability is plotted in Fig. 8 for the same parameters considered in Fig. 7.

V. Summary

This article has analyzed three different sync statistics based on measuring channel symbols. The performance of these three statistics was analyzed without statistical approximation for the basic tradeoff curves of miss probability and false-alarm probability. These basic performance curves were then extended to yield expressions for the probability of timely acquisition under two different acquisition strategies.

It was shown that the statistics based on decoded bits are superior to the statistics based on channel symbols if the desired operating region utilizes a miss probability many orders of magnitude higher than the false-alarm probability. This operating point is applicable for very large frame lengths and minimal frame-to-frame verification strategy. On the other hand, the statistics based on channel symbols are superior if the desired operating point has a miss probability only a few orders of magnitude greater than the false-alarm probability. This happens for small frames or when frame-to-frame verifications are required. Among the three channel symbol methods examined, the squared-distance statistic offers the best performance in the range of normal signal-to-noise ratios, but it degrades more rapidly than the correlation statistic or the hard-limited symbol discrepancy count statistic when the signal-to-noise ratio is extremely low.

"DATA" BITS {b_i}, INCLUDING
SYNC MARKER BITS {λ_i}

CONVOLUTIONAL
ENCODER

CONSTRAINT LENGTH K

CODE RATE 1/N

CHANNEL SYMBOLS {s_i}, INCLUDING
SYNC MARKER SYMBOLS {m_i}

CHANNEL

DECODED BITS {d_i}

MAXIMUM
LIKELIHOOD
CONVOLUTIONAL
DECODER

RECEIVED SYMBOLS {$r_i = s_i + n_i$}

SYNC MARKER BITS {λ_i, i = 1, ..., L} ARE TRANSMITTED ONCE EVERY DATA FRAME {b_i, i = 1, ..., B}

WITHIN EVERY SYMBOL FRAME {s_i, i = 1, ..., S} THE SYNC MARKER SYMBOLS {m_i, i = 1, ..., M}
ARE THOSE SYMBOLS THAT ARE COMPLETELY DETERMINED BY THE SYNC MARKER BITS

S = NB   M = N(L − K + 1)
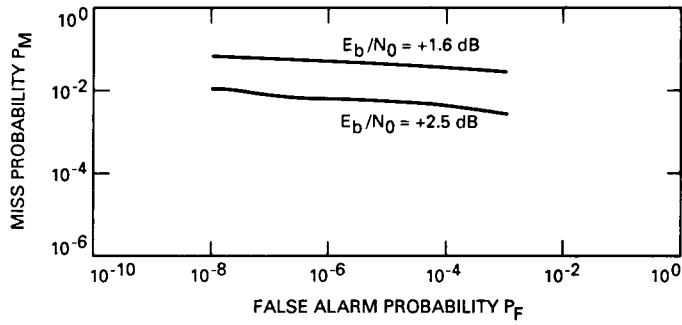
Fig. 1. System diagram for two sync methods.

**Fig. 2. P_M versus P_F for discrepancy count statistic
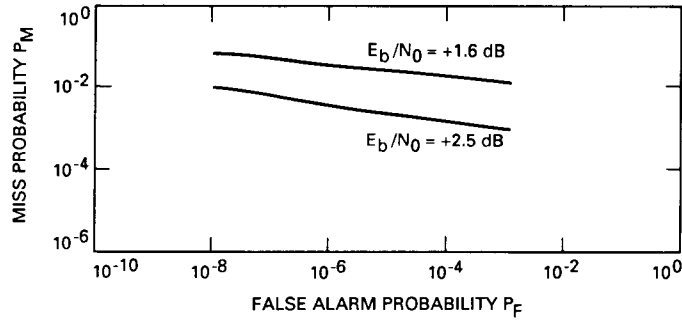based on decoded bits.**

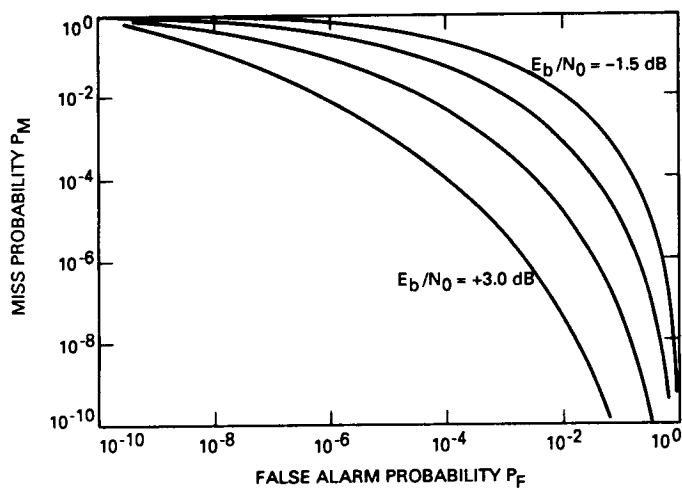**Fig. 3. P_M versus P_F for discrepancy span statistic
based on decoded bits.**

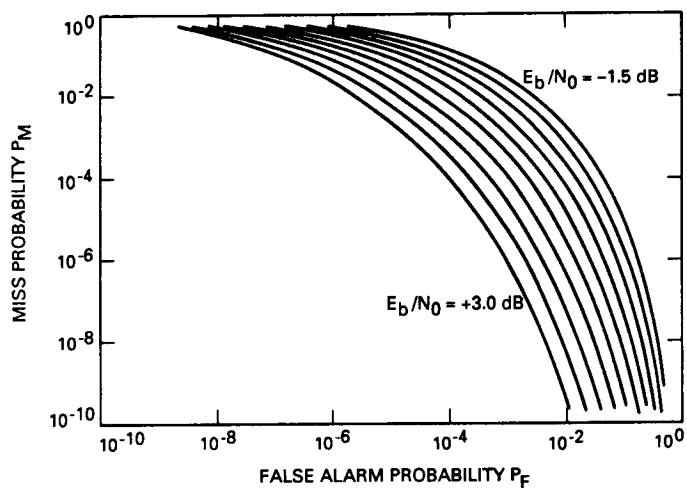Fig. 4. P_M versus P_F for hard-limited symbol discrepancies.

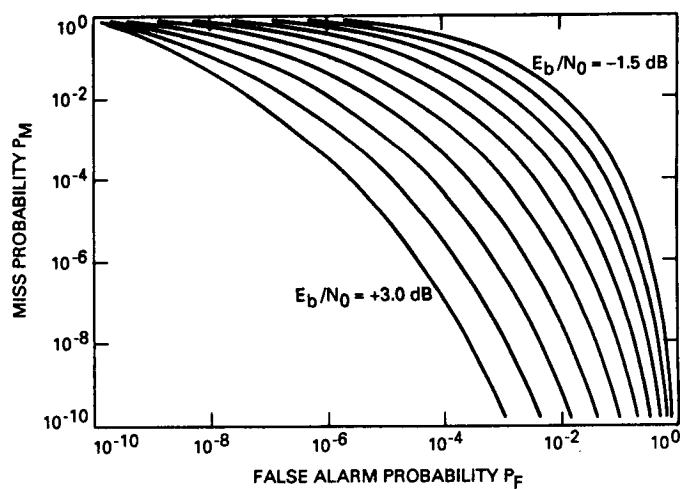Fig. 5. P_M versus P_F for correlation statistic.

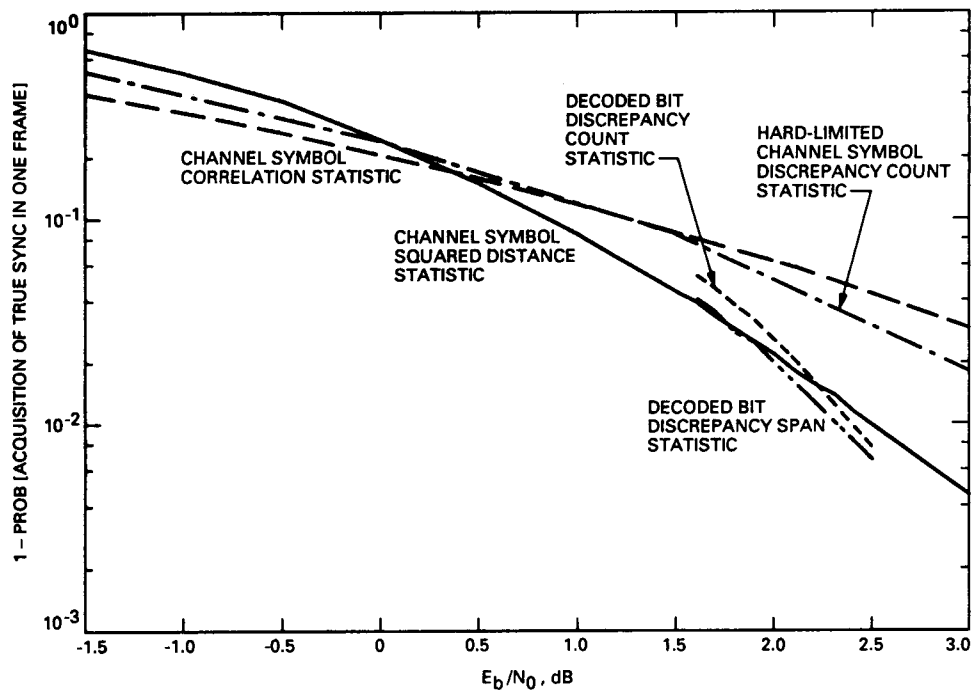Fig. 6. P_M versus P_F for squared-distance statistic.

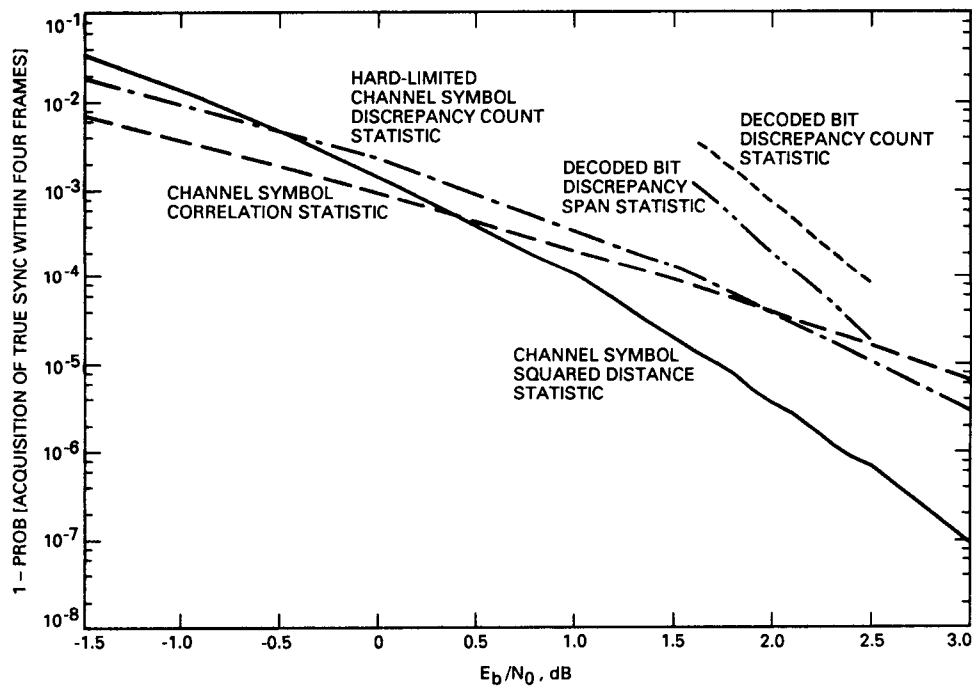Fig. 7. Probability of failure to acquire true sync within one 10000-bit frame.

Fig. 8. Probability of failure to acquire true sync within four 10000-bit frames, with required next-frame verification.

133

Appendix A

52-Symbol Weight Distribution for the NASA-Standard (7,1/2) Code

Evaluation of the false-alarm probabilities for the three channel symbol statistics analyzed in Section III requires knowledge of the probability distribution of the Hamming weights of the possible discrepancy sequences $\{\delta_i, i = 1, \ldots, M\}$ between the sync marker symbols $\{m_i, i = 1, \ldots, M\}$ and the sliding window of M symbols $\{s_i, i = 1, \ldots, M\}$ at the current location. The exact weight distribution for a 32-bit sync marker and the NASA-standard (7,1/2) code was generated by exhaustive enumeration. Since the convolutional code is linear, this weight profile is equivalent to the weight profile generated by encoding all possible 32-bit patterns. The 2^{32} possible bit patterns were encoded one by one, and a complete histogram of their encoded weights was produced. This process required about 14 days of CPU time on a Sun 3 computer.

It is shown in [5] and [6] that the weight distribution of a binary primitive block code is approximately binomial. Since the convolutional code is linear, and the 52-bit patterns represent truncated sequences from the output of the convolutional encoder, these 52-bit patterns can be regarded as the codewords of a (52,32) binary block code. Let A_w denote the number of patterns of weight w. Then according to [5] and [6] A_w can be approximated by the following binomial coefficient:

$$A_w \approx 2^{-20} \binom{52}{w} \equiv A'_w, \quad 0 \le w \le 52$$

A comparison between the exact weight distribution A_w and the approximate distribution A'_w is given in Table A-1. It is observed that A'_w is a good approximation to A_w except at the two extremes (w near 0 or 52).

Table A-1. Encoded weight profile for all possible 32-bit input sequences, encoded by the NASA-standard (7,1/2) code

Weight, w	Histogram totals		Ratio, A_w/A'_w
	Actual, A_w	Binomial, A'_w	
0	1	0	1048576.000
1	0	0	0.000
2	2	0	1581.563
3	7	0	332.128
4	18	0	69.718
5	40	2	16.138
6	122	19	6.284
7	333	128	2.610
8	963	718	1.342
9	3634	3509	1.036
10	14244	15087	0.944
11	54082	57605	0.939
12	191047	196819	0.971
13	600241	605596	0.991
14	1692962	1687018	1.004
15	4310848	4273778	1.009
16	9926772	9883112	1.004
17	20917283	20928944	0.999
18	40618430	40695169	0.998
19	72723310	72822934	0.999
20	120117817	120157841	1.000
21	183174400	183097662	1.000
22	258139236	258001251	1.001
23	336646298	336523371	1.000
24	406667062	406632406	1.000
25	455311348	455428295	1.000
26	472746296	472944768	1.000
27	455311348	455428295	1.000
28	406667062	406632406	1.000
29	336646298	336523371	1.000
30	258139236	258001251	1.001
31	183174400	183097662	1.000
32	120117817	120157841	1.000
33	72723310	72822934	0.999
34	40618430	40695169	0.998
35	20917283	20928944	0.999
36	9926772	9883112	1.004
37	4310848	4273778	1.009
38	1692962	1687018	1.004
39	600241	605596	0.991
40	191047	196819	0.971
41	54082	57605	0.939
42	14244	15087	0.944
43	3634	3509	1.036
44	963	718	1.342
45	333	128	2.610
46	122	19	6.284
47	40	2	16.138
48	18	0	69.718
49	7	0	332.128
50	2	0	1581.563
51	0	0	0.000
52	1	0	1048576.000
Total	2^{32}	2^{32}	

Appendix B

Relationship of Noncentral Chi-Squared Probability Distributions and Poisson Probability Distributions

Let ξ be a noncentral chi-squared random variable with M degrees of freedom and noncentrality parameter μ. Then, from [7], the probability distribution function of ξ can be expanded in the form

$$\text{Prob}[\xi > \theta] = \sum_{k=0}^{\infty} e^{-\mu/2} \frac{(\mu/2)^k}{k!} \text{Prob}[\xi_k > \theta]$$

where $\{\xi_k, k = 1, 2, \ldots\}$ are central chi-squared random variables with increasing numbers of degrees of freedom,

$$\xi_k \text{ is } \chi^2(M + 2k), \quad k = 1, 2, \ldots$$

Also from [7], the probability distributions for each of the central chi-squared random variables can be related to the Poisson distribution if M is even, according to

$$\text{Prob}[\xi_k > \theta] = \sum_{j=0}^{(M/2)+k-1} e^{-\theta/2} \frac{(\theta/2)^j}{j!}$$

These two results combine to yield

$$\text{Prob}[\xi > \theta] = \sum_{k=0}^{\infty} e^{-\mu/2} \frac{(\mu/2)^k}{k!} \sum_{j=0}^{(M/2)+k-1} e^{-\theta/2} \frac{(\theta/2)^j}{j!}$$

$$= \text{Prob}\left[j - k \leq \frac{M}{2} - 1\right]$$

where j and k are independent Poisson random variables with means $\theta/2$ and $\mu/2$, respectively.